Electron-acoustic solitary waves and double layers with an electron beam and phase space electron vortices in space plasmas

W. F. El-Taibany

Physics Department, Faculty of Science-Damietta, Mansoura University, Damietta El-Gedida, Egypt

Received 4 April 2004; revised 17 November 2004; accepted 24 November 2004; published 20 January 2005.

[1] The nonlinear propagation of electron acoustic waves (EAWs) in a plasma composed of a cold electron fluid, hot electrons obeying trapped/vortex-like distribution, warm electron beam, and stationary ions is considered. The streaming velocity of the beam, u_o, plays the dominant role in changing the topology of the linear dispersion relation. For small but finite amplitude EAWs, a modified Korteweg de Vries (MKdV) equation is derived. It is found that the MKdV supports EAWs having a positive potential, which corresponds to a hole (hump) in the cold (hot) electron number density. The energy soliton amplitude decreases, though its width increases for any increase in the beam parameters. In the vicinity of the isothermal population, a nonlinear evolution equation with mixed nonlinearity is obtained. Its solution gives a (compressive/rarefactive) soliton or a compressive double layer (DL) depending on the system parameters. For arbitrary amplitude EAWs, the exact Sagdeev potential has been derived. The admitted Mach number regime widens due to an increase of the beam parameters. With a better approximation in the Sagdeev potential, more features of solitary waves, e.g., spiky and explosive, are also highlighted. The introduced effects modify significantly the wave velocity, the amplitude, and the width of the EAWs investigated numerically. This theoretical model is in good agreement with the broadband noise emission observed by Geotail spacecraft in the plasma sheet boundary layer of the Earth's magnetosphere.

Citation: El-Taibany, W. F. (2005), Electron-acoustic solitary waves and double layers with an electron beam and phase space electron vortices in space plasmas, *J. Geophys. Res.*, *110*, A01213, doi:10.1029/2004JA010525.

1. Introduction

[2] Satellite measurements in the auroral and other regions of the magnetosphere have shown bursts of broadband electrostatic noise (BEN) emission with frequencies up to and higher than the electron plasma and cyclotron frequencies [*Temerin et al.*, 1982; *Matsumoto et al.*, 1994; *Catell et al.*, 1999]. The associated electric field intensities of these BENs range from a few μV/m to 100 mV/m. Observations of solitary waves in the auroral zone suggest that there are two classes of solitary waves: the first kind is associated with electron beams and the other is associated with ion beams [*Ergun et al.*, 1998]. Here the first kind will be the main focus.

[3] Solitary waves associated with electrons were first observed by Geotail [*Matsumoto et al.*, 1994] and later by FAST [*Ergun et al.*, 1998] and Polar [*Cattell et al.*, 1999]. The signature of these observations is found to display a nonlinear behavior. In particular, BEN is found to have waveforms of solitary bipolar electric field pulses which are called electrostatic solitary waves (ESW). The time-scale of ESW suggests that they are related to electron dynamic rather than ions [*Matsumoto et al.*, 1994]. *Onsager et al.* [1993] described the correlation of BEN with the high-energy electron component in the absence of ion flows. It is also found that these solitary waves in the plasma sheet boundary layer (PSBL) are either an electron hole (EH) or an electron acoustic solitary wave (EASW) propagating with velocities of a few thousand km/s [*Cattell et al.*, 1999]. The EH were first reported in laboratory experiments and numerical simulations and later analytically [*Saeki et al.*, 1979; *Schamel*, 1982; *Turikov*, 1984; *Guio et al.*, 2003]. These EHs are excited by a weak electron beam instability such as bump-on-tail instability, which is the most probable candidate that can form relatively small electrostatic potentials moving with the electron beam. These electrostatic potentials are formed by high-energy electrons in the nonlinear stage of electron beam instabilities reproduced in computer simulations [*Matsumoto et al.*, 1994; *Omura et al.*, 1994, 1996]. Moreover, they are close to the Bernstein-Green-Kruskal (BGK) equilibrium [*Bernstein et al.*, 1957] formed in the resonant and nonresonant plasma screenings of bunched electrons trapped by a potential pulse moving in a plasma [*Krasovsky et al.*, 1997]. The trapped electrons are responsible for the formation of the high-energy tail in the velocity distribution function [*Omura et al.*,

0148-0227/05/2004JA010525$09.00

1996]. The interaction of two weak ESWs associated with a deficit of the electrons trapped in the self-consistent potential well was studied by *Krasovsky et al.* [1999]. These authors showed that a violation of the adiabaticity of the particle motion and phase mixing process entail an irreversible deformation of the hole structure, effective heating of the holes, and the corresponding losses in the mechanical energy of the system. Recently, using the general analysis of localized BGK waves, *Krasovsky et al.* [2003] investigated unified physical models of ESW based on the additivity of the trapped electron distribution function as well as energetic relations and universal restrictions on the parameters and waveforms of the solitons.

[4] On the other hand, the spectrum of electron acoustic (EA) linear waves extends only up to the plasma frequency of the cold electron population, $\omega_{pc} = (4\pi e^2 n_{co}/m_e)^{1/2}$, where n_{co} is the unperturbed cold plasma density and m_e is the mass of electron. At this high frequency, the ion population plays the role of a neutralizing background, the restoring force comes from the pressure of the hot electrons, while the inertia comes from the mass of the cold electron component [*Watanabe and Taniuti*, 1977]. The EA velocity equals to $v_{ea} = (n_{co}/n_{ho})^{1/2} v_{th}$, where n_{ho} is the unperturbed hot electron density, $v_{th} = (K_B T_h/m_e)^{1/2}$, T_h is the hot electron temperature, and K_B is the Boltzmann's constant. *Tokar and Gary* [1984] found that electron acoustic waves (EAWs) contribute mostly to electrostatic high-frequency noise excited in a two-component electron plasma when the cold to hot electron population ratio is small. Later on, the relation between the higher-order modes and the EAWs in a two-electron-temperature plasma was discussed [*Mace and Hellberg*, 1990]. *Mace et al.* [1991] investigated the electron acoustic solitary waves (EASWs) in an unmagnetized plasma model in which the ions and the cold electron fluid are of finite temperature. However, their system admits the negative potential solitary structures associated only with a compression of the cold electron density.

[5] Since the EAWs can be excited by electron and laser beams [*Montgomery et al.*, 2001], the electron beams, in addition to the two electron populations, are considered to be the main energy source for the excitation of the wave mode. When the beam energy is sufficiently large, the nonlinear and dispersive effects will compete to produce EAWs, which are stationary in their comoving reference frame [*Watanabe and Taniuti*, 1977]. Motivated by the observations that the plasma in the Earth's magnetosphere consists of four species, *Berthomier et al.* [2000] studied EA solitons in an electron beam plasma system. The produced electrostatic potential pulses are associated with an enhancement of the cold electron density and a decrease of the hot electron density. *Singh and Lakhina* [2001] studied the generation of BEN by EAWs in a four-component unmagnetized plasma. They applied the linear theory to study the stability and the growth rate of the EAWs for three different regions of the Earth's magnetosphere.

[6] However, most of the previous studies are concerned only with a Maxwellian isothermal electron distribution. In practice, the hot electrons may not follow a Maxwellian distribution due to the formation of phase space holes caused by the trapping of hot electrons in a wave potential. Accordingly, in most space plasmas the hot electrons follow the trapped/vortex-like distribution [*Schamel*, 1972, 1979, 1986]. Recently, *Mamun and Shukla* [2002] studied EAWs in a space plasma system consisting of two-temperature electrons (the hot electrons obey the vortex-like distribution) and stationary ions using a Sagdeev potential method. It is found that the plasma model supports having a positive potential, which corresponds to a hole (hump) in the cold (hot) electron number density.

[7] The motive of this paper is to study the effect of the introduction of the fourth component (electron beam) into a three-component plasma system consisting of cold electron fluid, background warm electrons obeying vortex-like distribution, and stationary ions. The contribution of the hot electron distribution, whether they obey the vortex-like/trapped or the isothermal distributions, will be also studied. The present model is suggested to describe the ESW observed by Geotail spacecraft in the PSBL region.

[8] This paper is organized as follows: The basic equations governing the dynamics of the nonlinear EAWs are presented in section 2. In section 3 the evolution equation describing the propagation of nonlinear EAWs is derived. In section 4 a critical case, the Korteweg de Vries (KdV) equation with a mixed nonlinearity, is obtained. Its solutions and the conditions under which the double layer (DL) can be formed are discussed. In section 5 the exact Sagdeev potential is derived and the dependency of the admitted Mach number regime on the system parameters is investigated. Section 6 is devoted to the conclusion.

2. Basic Equations

[9] Let us consider a collisionless unmagnetized plasma with four components, namely, a cold electron fluid, hot electrons obeying trapped/vortex-like distribution, a warm electron beam, and stationary ions. The basic equations describing the propagation of the EAWs in dimensionless form are given as follows:

$$\frac{\partial n_j}{\partial t} + \frac{\partial (n_j u_j)}{\partial x} = 0, \tag{1}$$

$$\frac{\partial u_j}{\partial t} + u_j \frac{\partial u_j}{\partial x} + \alpha_c \left(3\sigma_j n_j \frac{\partial n_j}{\partial x} - \frac{\partial \phi}{\partial x} \right) = 0, \tag{2}$$

where n_j and u_j ($j = c$ for cold electron and b for electron beam) are the densities and velocities of the two fluids, ϕ is the electrostatic potential, x is the space coordinate, and t is the time variable. To model the hot electron distribution in the presence of trapped particles, we employ the following generalized vortex-like electron distribution, f_h, of *Schamel* [1972, 1973, 2000] which solves the electron Vlasov equation, i.e.,

$$f_{hf} = \frac{1}{\sqrt{2\pi}} \exp\left\{ -\frac{[\tilde{u} - (v_h - v_d)]^2}{2} \right\} \quad |u| > \sqrt{2\phi},$$

$$f_{ht} = \frac{1}{\sqrt{2\pi}} \exp\left\{ -\frac{\left[\beta \tilde{u} + (v_h - v_d)^2\right]}{2} \right\} \quad |u| \le \sqrt{2\phi},$$

where $\tilde{u} = \sqrt{(u - v_h)^2 - 2\phi}\ sign\ (u - v_h)$, v_d is the drift velocity of hot electron component and v_h is the velocity of vortices/holes which corresponds to the velocity of potential ϕ. $f_h = f_{hf} + f_{ht}$. Here f_{hf} represents the distribution of the untrapped electrons, which in the limit $\phi \rightarrow 0$ reduces to a shifted Maxwellian, as it should be. Here f_{ht} is the distribution function for the trapped electrons and represents a hole (in phase space) if β is negative. Here $|\beta|$ is the ratio of the free hot electron temperature T_h to the trapped electron temperature T_{ht} and it determines the number of trapped electrons. This distribution function is continuous in velocity space and satisfies the regularity requirements for an admissible BGK solution [*Schamel*, 1975]. As it is obvious, in the present physical model the cold fluid component and ions are in the rest frame, the electron beam component initially moving at u_o, the major hot component and vortices (i.e., potential structures) are moving at velocity equals to the EASW velocity λ. It is important to study propagation of EASWs in a realistic model in which potential structures are drifting against the major hot electrons motion, i.e., $v_h = v_d = \lambda$. Thus integrating the electron distributions over the velocity space, the hot electron number density n_h for $\beta < 0$ can be expressed as [*Schamel*, 1972, 1973]

$$n_h = I(\phi) + \frac{2}{\sqrt{\pi|\beta|}} W_D\left(\sqrt{-\beta\phi}\right), \tag{3a}$$

where $I(x) = [1 - erf(\sqrt{x})]\exp(x)$ and $W_D(x) = \exp(-x^2)\int_0^x \exp(y^2)\, dy$. Equation (3a) can be simplified to take the form

$$n_h = \exp(\phi) - G(\phi), \tag{3b}$$

where $G(\phi) = \sum_{k=1}^{\infty}[2^{(k+1)} b_k(\phi)^{(2k+1)/2}/\Pi(2k+1)]$, $b_k = (1 - \beta^k)/\sqrt{\pi}$. This system of equations is closed by Poissons's equation

$$\frac{\partial^2\phi}{\partial x^2} = \frac{n_c}{\alpha_c} + n_h + \frac{n_b}{\alpha_b} - \left(\frac{1}{\alpha_c} + \frac{1}{\alpha_b} + 1\right). \tag{4}$$

In equations (1)–(4), the physical quantities n_j, u_j, ϕ, x, and t are normalized to their equilibrium densities n_{jo} to v_{ea} to $K_B T_h/e$, to the hot electron Debye length $\lambda_{Dh} = (K_B T_h/4\pi n_{ho} e^2)^{1/2}$ and to ω_{pc}^{-1}, respectively. Also, we have introduced the following parameters

$$\alpha_j = \left(n_{ho}/n_{jo}\right)$$

and

$$\sigma_j = \left(T_j/T_h\right).$$

3. Nonlinear Electron Acoustic Waves (EAWs)

[10] In order to study the dynamics of small-amplitude EASWs, a reductive perturbation technique [*Washimi and Tanuiti*, 1966] is employed. First, we introduce the stretched coordinates [*Schamel*, 1972] $\xi = \varepsilon^{1/4}(x - \lambda t)$, and $\tau = \varepsilon^{3/4} t$ in equations (1)–(4), where ε is a small parameter. Here λ will be determined later. The physical quantities $\Psi \equiv [n_c, n_b, u_c, u_b, \phi]$ are expanded as power series in ε about their equilibrium values as

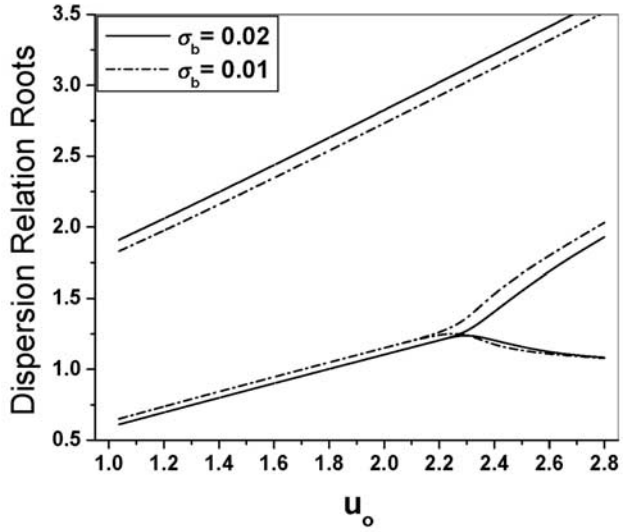

Figure 1. The dispersion relation roots against u_o for two different values of σ_b, where $\alpha_c = 5$, $\alpha_b = 15$, and $\sigma_c = 0.002$.

$$\Psi = \Psi_o + \sum_{q=1}^{\infty} \varepsilon^{\frac{q+1}{2}} \Psi_q. \tag{5}$$

We assume the following boundary conditions, as $|\xi| \rightarrow \infty$

$$\begin{aligned} n_j &\longrightarrow 1, \\ u_c &\longrightarrow 0, \\ u_b &\longrightarrow u_o, \\ \phi &\longrightarrow 0. \end{aligned} \tag{6}$$

[11] Substituting these expansions into the basic set of equations (1)–(4), then collecting terms with different powers of ε, we obtain to the lowest order

$$\begin{aligned} &n_{c1} = -\alpha_c Z_1 \phi_1,\ u_{c1} = -\lambda\alpha_c Z_1\, \phi_1,\ n_{b1} = -\alpha_c Z_2 \phi_1, \\ &u_{b1} = -\tilde{\lambda}\,\alpha_c Z_2\, \phi_1, \end{aligned} \tag{7}$$

where

$$Z_1 = \left(\lambda^2 - 3\alpha_c\sigma_c\right)^{-1},\ Z_2 = \left(\tilde{\lambda}^2 - 3\alpha_c\sigma_b\right)^{-1},\ \tilde{\lambda} = \lambda - u_o.$$

The linear dispersion relation is given by

$$Z_1 + (\alpha_c/\alpha_b) Z_2 = 1. \tag{8}$$

Equation (8) is a fourth-order algebraic equation in λ from which one can get the wave velocity λ that will present the lowest admitted Mach number for the present system. We can observe that λ is independent of β and it agrees exactly

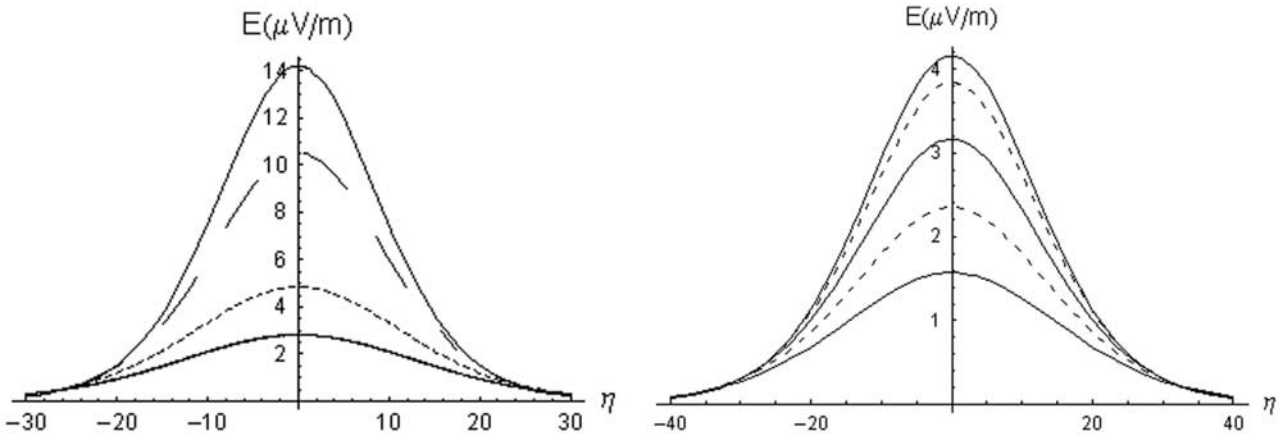

Figure 2. The variation of E and its width with η; (a) $\alpha_b = 15$, $\sigma_b = 0.02$, $u_o = 1.72$ (solid), 1.73 (dashed),1.75 (dotted), 1.76 (thick solid) with $\lambda = 1.74$; and (b) $\alpha_b = 10$, $\sigma_b = 0.02$ (label 1), $\alpha_b = 15$, $\sigma_b = 0.018$ (label 2), $\alpha_b = 15$, $\sigma_b = 0.02$ (label 3), $\alpha_b = 15$, $\sigma_b = 0.022$ (label 4), $\alpha_b = 20$, $\sigma_b = 0.02$ (label 5) with $\lambda = 1.72$, $u_o = 1.74$, where $\beta = -0.75$, $\nu = 0.1$, $\alpha_c = 5$, $\sigma_c = 0.002$. The curves are labeled from bottom to top with 1, 2, ..., 5, respectively.

with that obtained by *Berthomier et al.* [2000] and *Mamun and Shukla* [2002]. However, *Mamun and Shukla* [2002] considered that the wave velocity equals to one. It was registered from the results of auroral observations of BEN that the EAWs propagate with a supersonic velocity, i.e., greater than v_{ea}. In this model, the introduction of the warm electron beam with the inclusion of the temperature of each species changes the topology of the root of equation (8) and overcomes this discrepancy. Figure 1 shows the dependency of the positive roots of equation (8) on u_o for two values of σ_b. It is obvious that λ increases as u_o increases. *Singh and Lakhina* [2001] predicted that the maximum growth rate of the EAWs took place at $u_o = 2.2$, after which (8) will admit three different wave velocities. Moreover, λ is affected by σ_b variation but it is not affected significantly by σ_c change. The parameters are chosen in this paper to compare our results with the ESW observed in the PSBL region [*Parks*, 1984; *Onsager et al.*, 1993; *Singh and Lakhina*, 2001; *Omura et al.*, 1994, 1999; *Matsumoto et al.*, 1994].

[12] To the next higher order in ε, we get a system of equations in the second-order perturbed quantities. Solving this system and with the aid of equation (7), we finally obtain the modified Korteweg de Vries (MKdV) equation

$$\frac{\partial \phi_1}{\partial \tau} + \frac{4 b_1 A}{3} \frac{\partial \phi_1^{3/2}}{\partial \xi} + A \frac{\partial^3 \phi_1}{\partial \xi^3} = 0, \tag{9}$$

where

$$A = \left[2 \left(\lambda Z_1^2 + \frac{\alpha_c}{\alpha_b} \tilde{\lambda} Z_2^2 \right) \right]^{-1}.$$

Using $\eta = \xi - \nu\tau$ and the boundary conditions

$$\phi_1(\eta) \to 0, \ \frac{d\phi_1(\eta)}{d\eta} \to 0, \ \frac{d^2\phi_1(\eta)}{d\eta^2} \to 0 \ as \ |\eta| \to \infty, \tag{10}$$

the stationary solution of equation (9) is given by

$$\phi_1 = \phi_{1m} Sech^4[(\xi - \nu\tau)/w_1], \tag{11}$$

where the amplitude ϕ_{1m} and the width w_1 are given by $(15\nu/16 b_1 A)^2$ and $4\sqrt{A/\nu}$, respectively. Here ν is an arbitrary parameter similar to a Mach number which allows the possibility of solitons moving with velocity to differ from the phase velocity of the wave [*Tagare et al.*, 2004]. Equation (11) reveals the existence of small but finite amplitude EASWs with a positive potential only, i.e., a hump in the hot electron number density. This corresponds to the rarefaction of the cold electron density, i.e., the cold electron density holes since $n_{c1} = -\alpha_c Z_1 \phi_1$. As ν increases, the amplitude increases but the width decreases. The choice of ESW parameters observed in the PSBL leads to $\lambda_{Dh} \simeq 607.277$ m. Thus using the formula $E = \phi_m (K_B T_h / e\lambda_{Dh}) \simeq \phi_m (1000/607.27)$ V/m, the solution (11) can be transformed into the energy form. Figure 2a shows the variation of the admitted compressive energy soliton whatever λ lower or higher than u_o to compare easily with the numerical study of *Omura et al.* [1994, 1996] who considered λ is slower than u_o. For a fixed λ the amplitude E decreases as u_o increases, but its width increases, and vice versa, for a fixed u_o and changes occurred in λ (not shown). In addition, as α_b or σ_b increases, the amplitude E decreases though the width increases. The effect of increasing $|\beta|$ is verified as *Mamun and Shukla* [2002] did but is not shown. It has the same effect as α_b.

4. Critical Case

[13] The propagation of compressive solitons solution (11) depends on the sign of the nonlinear coefficient of the MKdV equation. The necessary condition for the soliton existence is for the dispersion coefficient of the MKdV equation to be positive, otherwise no soliton will exist. When the nonlinear coefficient equals to zero, equation (9)

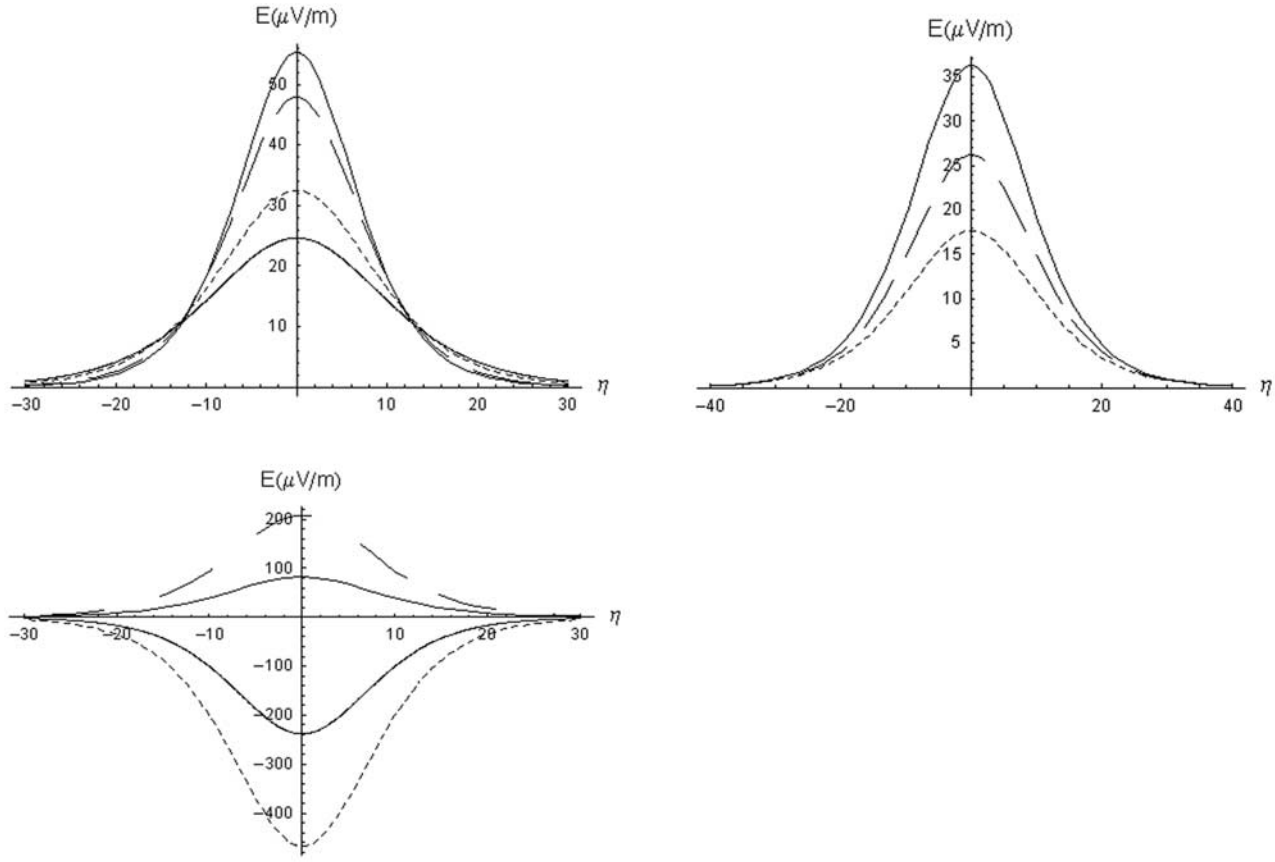

Figure 3. The variation of E and its width with η; (a) the parameters are chosen as in Figure 2a; (b) α_b = 15, σ_b = 0.022 (solid), 0.02 (dashed), 0.018 (dotted), and in (c) α_b = 30 (solid), α_b = 50 (dashed), α_b = 200 (dotted), no beam (thick solid) where u_o = 1.74, λ = 1.72 and the remainder parameter as in Figure 2.

fails to describe the system. This circumstance can be done if $b_1 = 0$, i.e. all particles obey the isothermal population. In this case, one has to seek another equation suitable for describing the evolution of the system. Using the stretching coordinates [*Washimi and Tanuiti*, 1966] $\xi = \varepsilon^{1/2}(x - \lambda t)$, and $\tau = \varepsilon^{3/2}t$, and following the same procedure used before, we obtain the same relations as equation (7) for the lowest order of ε, and for $\varepsilon^{3/2}$, we get the second-order perturbed quantities as

$$n_{c2} = -\alpha_c Z_1 \phi_2,\ u_{c2} = -\lambda \alpha_c Z_1 \phi_2, n_{b2} = -\alpha_c Z_2 \phi_2,$$
$$u_{b2} = -\tilde{\lambda} \alpha_c Z_2 \phi_2, \phi_2 = 4 b_1 \phi_1^{3/2} / \{3[1 - Z_1 - (\alpha_c/\alpha_b) Z_2]\}. \quad (12)$$

If we consider the next-order $O(\varepsilon^2)$, we obtain a system of equations that yields, with the aid of equations (7) and (12),

$$\frac{\partial \phi_1}{\partial \tau} + 2 b_1 A \frac{\partial \phi_1^{1/2} \phi_2}{\partial \xi} + A \frac{\partial^3 \phi_1}{\partial \xi^3} + B \frac{\partial \phi_1^2}{\partial \xi} = 0, \quad (13)$$

where

$$B = (-A/2)\left\{1 + 3\alpha_c \left[Z_1^3 (\alpha_c \sigma_c + \lambda^2) + \frac{\alpha_c}{\alpha_b} Z_2^3 (\alpha_b \sigma_b + \tilde{\lambda}^2)\right]\right\}.$$

The solution of this equation with $b_1 = 0$, using the boundary conditions (10), is given by

$$\phi_1 = \phi_{2m}\, Sech^2\, [(\xi - \nu\tau)/w_2], \quad (14)$$

where the amplitude ϕ_{2m} and the width w_2 are given here by $3\nu/2B$ and $2\sqrt{A/\nu} = 0.5\ w_1$, respectively. Since $\nu > 0$, equation (14) admits mathematically the existence of either compressive or rarefactive soliton waves depending on the sign of B. However, as shown in Figure 3, the rarefactive soliton will appear only for a very low electron beam density or for a three-component plasma, i.e., without electron beam. On the other hand, if the amplitude becomes negative (rarefactive) for other values of system parameters, the width of the soliton will be imaginary and the soliton solution is forbidden.

[14] Comparing the KdV and MKdV solutions, it is clear that the width of the KdV soliton equals to half of the MKdV soliton's width, i.e., the width will be narrower if the particles have an isothermal population. Though, the energy amplitude E for the isothermal case is larger than the vortex-like electron case. The effect of u_o, λ, and σ_b variation on both E and its width has the same feature that occurred in the MKdV case. Moreover, the parameter α_b plays the dominant role for rarefactive soliton appearance. For $\alpha_b >$

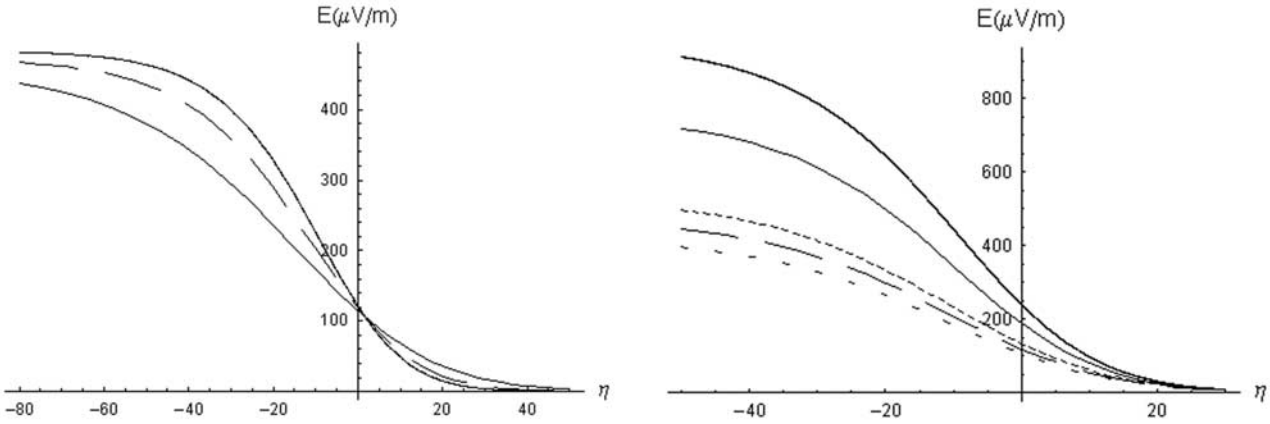

Figure 4. The variation of E and its width with η; (a) $\alpha_b = 15$, $\sigma_b = 0.02$, $\lambda = 1.74$, $u_o = 1.78$ (solid), 1.77 (dashed), 1.76 (thick curve); (b) $\alpha_b = 15$, $\sigma_b = 0.022$ (solid) and 0.02 (dashed) with $\beta = -0.75$ and $\sigma_b = 0.02$, $\beta = -0.85$(dotted), $\beta = -0.65$ (lower curve), $\alpha_b = 20$, $\beta = -0.75$ (thick solid) where $u_o = 1.75$ and $\lambda = 1.72$ and the remainder parameter as in Figure 2.

100, the solution becomes a rarefactive one, otherwise, it has a compressive character. This result agrees with what was stated previously [*Omura et al.*, 1994, 1999; *Matsumoto et al.*, 1999] as the condition for ESW formation in the PSBL, namely that the beam must have a minor density ratio with respect to the total electron density. For compressive (rarefactive) soliton, as α_b increases, E increases (decreases) and its width decreases (increases).

[15] On the other hand, when $b_1 \to 0$, equation (13) would reduce to

$$\frac{\partial \phi_1}{\partial \tau} + 2b_1 C \phi_1^{1/2} \frac{\partial \phi_1}{\partial \xi} + A \frac{\partial^3 \phi_1}{\partial \xi^3} + B \frac{\partial \phi_1^2}{\partial \xi} = 0, \qquad (15)$$

where we have used $A\phi_2 \to 2C\phi_1/3$ [*El-Labany and El-Taibany*, 2003]. If C is of O(1), then 1/4 scaling prevails accounting for a balance of the increased nonlinearity and dispersion. On the other hand, if C is O($\varepsilon^{1/2}$), the nonlinearity is weakened and becomes comparable to the ordinary hydrodynamic nonlinearity represented by the nonlinear term and the 1/2 scaling is appropriate. So, the scaling reflects the strength of the nonlinearity which is accounting for different solitary wave solutions [*Schamel*, 1972]. Equation (15) has a DL solution of the form

$$\phi_1 = \phi_m \{1 - Tanh[(\xi - \nu\tau)/w]\}^2, \qquad (16)$$

with

$$\phi_m = \left(\frac{2b_1 C}{5B}\right)^2,$$

$$\nu = \frac{-1}{6B}\left(\frac{8b_1 C}{5}\right)^2,$$

and

$$w = \frac{5\sqrt{-6BA}}{2Cb_1}. \qquad (17)$$

It is clear that only the compressive EA DLs are admitted for the present system. As known from the DLs properties, they constitute a second type of nonlinear coherent structures in a plasma. The associated electric field is able to speed up/slow down particles in narrow spatial regions to many kilovolts. It was considered as one of the major acceleration mechanisms occurring in nature [*Schamel*, 1982]. A DL is defined as a monotonic transition of the electric potential connecting smoothly two differently biased plasmas [*Schamel*, 1986]. The transition from a high energy level to a lower one, as the wave propagates (η increases), is investigated in Figure 4. It shows that for u_o greater than λ, by increasing u_o, the amplitude of the compressive DL decreases roughly, but its width increases. On the other hand, for $u_o < \lambda$ the amplitude increases but its width decreases (not shown). As α_b, σ_b or $|\beta|$ increases, E increases even though its width decreases.

5. Sagdeev Potential

[16] To investigate the properties of arbitrary amplitude EASWs. We assume that all variables in equations (1)–(4) depend only on a single variable $\zeta = x - Mt$, where ζ is normalized by λ_{Dh} and M is the Mach number. In this stationary frame, equations (1) and (2) can be integrated to give

$$n_b = \frac{1}{\sqrt{1 + \left\{2\alpha_c \phi \Big/ \left[(M - u_o)^2 - 3\alpha_c \sigma_b\right]\right\}}}$$

and

$$n_c = \frac{1}{\sqrt{1 + [2\alpha_c \phi/(M^2 - 3\alpha_c \sigma_c)]}}, \qquad (18)$$

where we have imposed the appropriate boundary conditions for localized disturbances, namely, $\phi \to 0$, $n_b \to 1$, $n_c \to 1$, $u_c \to 0$, $u_b \to u_o$ as $\zeta \to \pm\infty$.

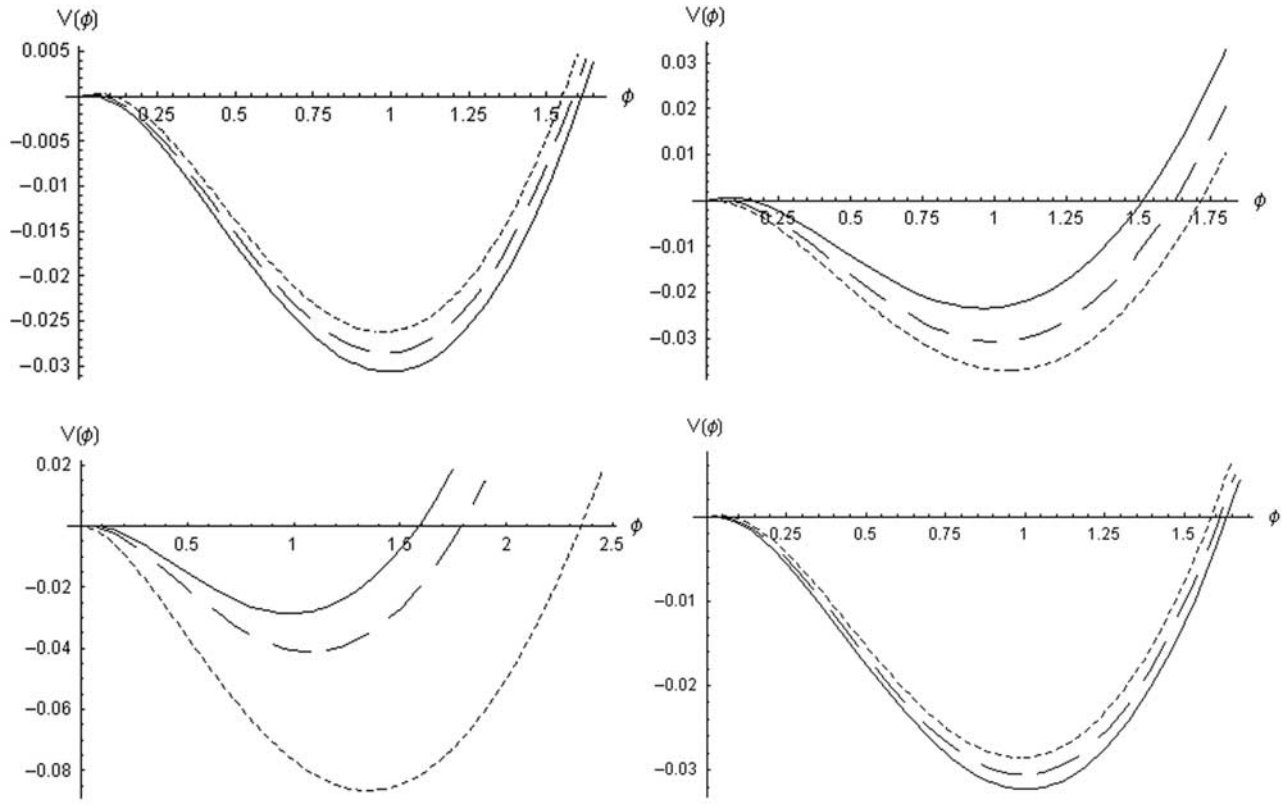

Figure 5. The variation of the Sagdeev Potential with ϕ, (a) $\alpha_b = 15$, $\sigma_b = 0.02$, M = 2.5, $\beta = -0.75$, $u_o = 1.7$ (solid), 1.75(dashed), 1.8 (dotted); (b) $\alpha_b = 15$, $\sigma_b = 0.02$, $u_o = 1.85$, $\beta = -0.75$, M = 2.5 (solid), 2.6 (dashed), 2.7 (dotted); (c) $\sigma_b = 0.02$, $u_o = 1.75$, $\beta = -0.75$, M = 2.5, $\alpha_b = 15$ (solid), 20 (dashed), no beam (dotted); and (d) $\alpha_b = 15$, $u_o = 1.85$, $\beta = -0.75$, M = 2.5, $\sigma_b = 0.01$ (solid), 0.015 (dashed), 0.02 (dotted) with $\alpha_c = 5$ and $\sigma_c = 0.002$.

[17] Substituting for the normalized number densities of hot, cold electrons, and electron beam into Poisson equation (4) and integrating once, imposing the boundary conditions for localized solutions; equation (10), we get

$$\frac{1}{2}\left(\frac{d\phi}{d\zeta}\right)^2 + V(\phi) = 0 \tag{19}$$

$$\begin{aligned} V(\phi) = {} & \frac{1}{\alpha_c \alpha_b}\left[(M-u_o)^2 - 3\alpha_c\sigma_b\right] \\ & \cdot\left(1 - \sqrt{1 + \left\{2\alpha_c\,\phi \Big/ \left[(M-u_o)^2 - 3\alpha_c\,\sigma_b\right]\right\}}\right) + 1 \\ & + \frac{1}{\alpha_c^2}\left(M^2 - 3\alpha_c\sigma_c\right)\left\{1 - \sqrt{1 + [2\alpha_c\,\phi/(M^2 - 3\alpha_c\sigma_c)]}\right\} \\ & + \phi\left(\frac{1}{\alpha_c} + \frac{1}{\alpha_b} + 1\right) - \exp(\phi)\left[1 - erf\left(\sqrt{\phi}\right)\right]\Big\} \\ & - \frac{2}{\sqrt{\pi\,\beta^3}}\exp(\beta\phi)\int_0^{\sqrt{-\beta\phi}}\exp(y^2)\,dy + 2\sqrt{\frac{\phi}{\pi}}\left(\frac{1}{\beta} - 1\right). \end{aligned} \tag{20}$$

[18] In order to have solitary wave solutions, the quasi-potential must satisfy the following conditions, (1) $V(\phi) \to 0$, $\frac{dV(\phi)}{d\phi} \to 0$ and $\frac{d^2V(\phi)}{d\phi^2} < 0$ at $\phi = 0$; i.e., the fixed point at the origin is unstable; (2) there exists a nonzero ϕ_m, the maximum (or minimum) value of ϕ, at which $V(\phi_m) \geq 0$; and (3) $V(\phi) < 0$ when ϕ lies between 0 and ϕ_m. From equation (20), condition 1 leads to an equation similar to (8) that fixes the lower limit of M, which is equivalent to the value of λ obtained in section 3. The upper limit of M for which solitary waves exist can be found from the condition $V(\phi_{\min}) = 0$, where $\phi_{\min}$ is the minimum value of ϕ for which n_c and n_b are real, i.e., $\phi < [(3\alpha_c\sigma_b - (M-u_o)^2)]/2\alpha_c$ and $\phi < (3\alpha_c\sigma_c - M^2)/2\alpha_c$.

[19] Figure 5 shows the variation of the Sagdeev potential corresponding to system parameters changes. One can easily observe the variation of both $\phi_{\max}$ and $V_{\min}$ (minimum value of the Sagdeev potential), where $\phi_{\max}$ is the value of ϕ, at which $V(\phi)$ intersects the ϕ-axis. Now, using the formula of the predicted energy E, λ_{Dh} and $\Delta = \phi_{\max}/\sqrt{|V_{\min}|}$, [*Bujarbarua and Schamel*, 1981], where Δ is the width of the EASWs, one can easily calculate exactly the amplitude, the velocity, and the width of any arbitrary amplitude EASWs. The critical upper limit of Mach number M_{cr} for which positive plasma potential solitary

waves exist can be found from the condition $V(\phi_{max}) = 0$, i.e., ϕ_{max} and M_{cr} should be determined from the coupled transcendental relations

$$\frac{1}{\alpha_c\alpha_b}\left[(M-u_o)^2-3\alpha_c\sigma_b\right]\cdot\left(1-\sqrt{1+\left\{2\alpha_c\,\phi\Big/\left[(M-u_o)^2-3\alpha_c\,\sigma_b\right]\right\}}\right)+1+\frac{1}{\alpha_c^2}\left(M^2-3\alpha_c\sigma_c\right)\left\{1-\sqrt{1+[2\alpha_c\,\phi/(M^2-3\alpha_c\sigma_c)]}\right\}+\phi\left(\frac{1}{\alpha_c}+\frac{1}{\alpha_b}+1\right)-\exp(\phi)\left[1-erf\left(\sqrt{\phi}\right)\right]\Big\}-\frac{2}{\sqrt{\pi\,\beta^3}}\exp(\beta\phi)\int_0^{\sqrt{-\beta\phi}}\exp(y^2)dy+2\sqrt{\frac{\phi}{\pi}}\left(\frac{1}{\beta}-1\right)=0 \tag{21}$$

and

$$\frac{1}{\sqrt{1+2\alpha_c\,\phi\Big/\left[(M-u_o)^2-3\alpha_c\sigma_b\right]}}+\frac{1}{\sqrt{1+2\alpha_c\,\phi/(M^2-3\alpha_c\sigma_c)}}+I(\phi)+\frac{2}{\sqrt{\pi|\beta|}}W_D\left(\sqrt{-\beta\phi}\right)-\left(\frac{1}{\alpha_c}+\frac{1}{\alpha_b}+1\right)=0 \tag{22}$$

[20] Figure 6 shows the dependence of the maximum Mach number, M_{max}, on u_o and σ_b variations. M_{max} increases as u_o or σ_b increases, i.e., the beam parameter increase will widen the admitted velocity regime of the present system.

[21] Since the expression for $V(\phi)$ derived in equation (20) is exact, one can expand it up to any desired power of ϕ and then can obtain all different types of solitary waves (solitons, DL, collapsive, and spiky solitons) obtained by the perturbation theory in the previous two sections. Using the tanh method [*Das et al.*, 1998], if we expand the expression for quasi-potential around $\phi = 0$, for $O(\phi^{7/2})$, we can get

$$V(\phi)=\frac{\phi^2}{2}\left\{(M-3\alpha_c\sigma_c)^{-1}+(\alpha_c/\alpha_b)\left[(M-u_o)^2-3\alpha_c\sigma_b\right]^{-1}-1\right\}+\frac{8}{15}b_1\phi^{5/2}-\frac{\phi^3}{6}\left(1+3\left\{\frac{\alpha_c}{(M^2-3\alpha_c\sigma_c)^2}+\frac{\alpha_c^2}{\alpha_b\left[(M-u_o)^2-3\alpha_c\sigma_b\right]^2}\right\}\right)+\frac{16b_2\phi^{7/2}}{105}.$$

In this case, equation (19) becomes

$$\left(\frac{d\phi}{d\zeta}\right)^2=a_1\phi^2-a_2\phi^{5/2}-a_3\phi^3-a_4\phi^{7/2}, \tag{23}$$

where $a_1 = -\{(M-3\alpha_c\sigma_c)^{-1}+(\alpha_c/\alpha_b)[(M-u_o)^2-3\alpha_c\sigma_b]^{-1}-1\}$, $a_2=\frac{16b_1}{15}$, $a_3=\frac{1}{3}+\{\frac{\alpha_c}{(M^2-3\alpha_c\sigma_c)^2}+\frac{\alpha_c^2}{\alpha_b\left[(M-u_o)^2-3\alpha_c\sigma_b\right]^2}\}$ and $a_4=\frac{32b_2}{105}$. If $a_2 = a_3 = 0$, we have the soliton solution

$$\phi=\phi_{3m}Sech^{4/3}[\zeta/w_3],$$

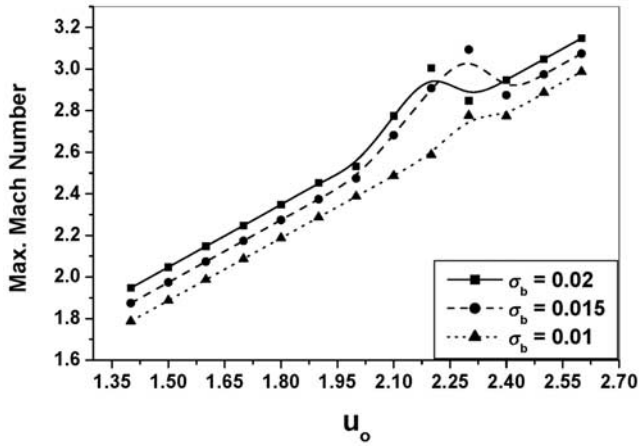

Figure 6. The variation of M_{max} with u_o for different σ_b where $\alpha_c = 5$, $\alpha_b = 15$, $\sigma_c = 0.002$, and $\beta = -0.75$.

where the amplitude ϕ_{3m} and the width w_3 are given by $(a_1/a_4)^{2/3}$and $\sqrt{16/9a_1}$, respectively. On the other hand, we can reform equation (23), using $\phi = \theta^2$, as

$$\left(\frac{d\theta}{d\zeta}\right)^2=a\theta^2(F-\theta)^3, \tag{24}$$

where $F = -a_3/3a_4$, $a = a_4/4$ and $a_3^2 = 3a_2a_4$. Equation (24) can be solved for the soliton profile and the solution can be obtained as an implicit function of ζ in the following form

$$\phi(\zeta)=F^2\left(1-Tanh^2\left\{\left[\frac{F}{F-\sqrt{\phi(\zeta)}}\right]^{1/2}-\sqrt{aF^3}\frac{\zeta}{2}\right\}\right)^2. \tag{25}$$

This solution gives a profile of spiky solitary waves defined in the region $0 < \phi(\zeta) < \sqrt{F}$ and is affected by $a_1$and a_3 which are functionally dependent on the electron beam and the fluids temperatures, as well as by trapped electrons through a_2 and a_4. On the other hand, for the region defined by $\phi < 0$, the soliton solution can be obtained in a similar manner and it has an explosive solitary wave profile in the plasma acoustic dynamics. Following the same procedure and taking higher nonlinear terms, a more complicated implicit function that contains the same features as equation (25) can be obtained [*Das et al.*, 1998; *El-Labany and El-Taibany*, 2003]. Now, we can describe EASWs, DLs, and other solitary structures and can fully describe any ESWs observed in the PSBL recorded by Geotail or the BEN emissions observed in the dayside auroral region.

6. Conclusion

[22] The nonlinear propagation of EAWs in a plasma composed of a cold electron fluid, hot electrons obeying a trapped/vortex-like distribution, warm electron beam, and stationary ions is investigated. The properties of small as well as arbitrary amplitude EASWs are studied by employing the reductive perturbation and the quasipotential techniques. The combined effects of the warm electron beam,

the fluid temperatures, and the vortex-like electron distribution modifies significantly the wave velocity, the amplitude, and the width of the EAWs. The linear dispersion relation reveals that as u_o increases, the topology of its roots is changed, which agrees with the work of *Berthomier et al.* [2000] and *Singh and Lakhina* [2001]. From the nonlinear point of view, a modified Korteweg de Vries (MKdV) equation (9), adequate for describing the system up to the first-order perturbed electrostatic potential, is derived. It admits only compressive solitons which represent a hump (hole) in the hot (cold) electron density. As the nonisothermal population decreases, i.e., most of the electrons have an isothermal distribution, the system is governed by an evolution equation with mixed nonlinearity, equation (13). Depending on the system parameter choice, equation (13) leads to compressive DL, (16), or soliton solution, (14), with the possibility of both kinds. The beam density ratio parameter plays the dominant role for rarefactive soliton appearance.

[23] Employing the quasipotential technique, all the previous results derived by the reductive perturbation technique plus other solitary wave solutions, like spiky and explosive soliton solutions, are obtained by a proper choice of the electrostatic potential when deriving the Sagdeev potential of the system.

[24] The variation of the energy amplitude, width, and the wave velocity of different cases are numerically investigated. To get some realistic appreciation of the present theoretical model, it is applied to the geophysical observation registered by Geotail spacecraft in the PSBL region. It was predicted that the observed energy range is 10 μV/m to 500 μV/m [*Omura et al.*, 1994, 1996, 1999; *Matsumoto et al.*, 1994]. So, it is evident through the numerical investigation that this model has a good agreement with the observed BENs in this region with different situations. Moreover, it can be considered as a generalization of the simple model presented by *Mamun and Shukla* [2002] when describing BENs observed in the dayside auroral region of the Earth's magnetosphere [*Dubouloz et al.*, 1991].

[25] **Acknowledgment.** Shadia Rifai Habbal thanks Takayuki Umeda and another referee for their assistance in evaluating this paper.

References

Bernstein, I. B., J. M. Greene, and M. D. Kruskal (1957), Exact nonlinear plasma oscillations, *Phys. Rev.*, *108*, 546–550.

Berthomier, M., R. Pottelette, M. Malingre, and Y. Khotyainsev (2000), Electron acoustic solitons in an electron-beam plasma system, *Phys. Plasmas*, *7*, 2987–2994.

Bujarbarua, S., and H. Schamel (1981), Theory of finite-amplitude electron and ion holes, *J. Plasma Phys.*, *25*, 515–629.

Cattell, C. A., et al. (1999), Comparisons of Polar satellite observations of solitary wave velocities in the plasma sheet boundary and the high altitude cusp to those in the auroral zone, *Geophys. Res. Lett.*, *26*, 425–428.

Das, G. S., J. Sarma, and M. Talukdar (1998), Dynamical aspects of various solitary waves and double layers in dusty plasmas, *Phys. Plasmas*, *5*, 63–69.

Dubouloz, N., R. Pottelette, M. Malingre, and R. A. Treumann (1991), Generation of broadband electrostatic noise by electron acoustic solitons, *Geophys. Res. Lett.*, *18*, 155–158.

El-Labany, S. K., and W. F. El-Taibany (2003), Dust acoustic solitary waves and double layers in a dusty plasma with trapped electrons, *Phys. Plasmas*, *10*, 4685–4695.

Ergun, R. E., et al. (1998), FAST satellite observations of large-amplitude solitary structures, *Geophys. Res. Lett.*, *25*, 2041–2044.

Guio, P., et al. (2003), Phase space vortices in collisionless plasmas, *Nonlinear Proc. Geophys.*, *10*, 75–86.

Krasovsky, V. L., H. Matsumoto, and Y. Omura (1997), Bernstein-Greene-Kruskal analysis of electrostatic solitary waves observed with Geotail, *J. Geophys. Res.*, *102*, 22,131–22,140.

Krasovsky, V. L., H. Matsumoto, and Y. Omura (1999), Interaction of small phase density holes, *Phys. Scr.*, *60*, 438–451.

Krasovsky, V. L., H. Matsumoto, and Y. Omura (2003), Electrostatic solitary waves as collective charges in a magnetospheric plasma: Physical structure and properties of Bernstein Greene Kruskal (BGK) solitons, *J. Geophys. Res.*, *108*(A3), 1117, doi:10.1029/2001JA000277.

Mace, R. L., and M. A. Hellberg (1990), Higher-order electron modes in a two-electron-temperature plasma, *J. Plasma Phys.*, *43*, 239–255.

Mace, R. L., S. Baboolal, R. Bharuthram, and M. A. Hellberg (1991), Arbitrary amplitude electron acoustic solitons in a two-electron-component plasma, *J. Plasma Phys.*, *45*, 323–338.

Mamun, A. A., and P. K. Shukla (2002), Electron-acoustic solitary waves via vortex electron distribution, *J. Geophys. Res.*, *107*(A7), 1135, doi:10.1029/2001JA009131.

Matsumoto, H., H. Kojima, T. Miyatake, Y. Omura, M. Okada, I. Nagano, and M. Tsutui (1994), Electrostatic solitary waves (ESW) in the magnetotail: BEN wave forms observed by Geotail, *Geophys. Res. Lett.*, *21*, 2915–2918.

Matsumoto, H., et al. (1999), Generation mechanism of ESW based on Geotail plasma wave observation, plasma observation and particle simulation, *Geophys. Res. Lett.*, *26*, 421–424.

Montgomery, D. S., R. J. Focia, H. A. Rose, D. A. Russell, J. A. Cobble, J. C. Fernañdez, and R. P. Johnson (2001), Observation of stimulated electron acoustic wave scattering, *Phys. Rev. Lett.*, *87*, 15.

Omura, Y., H. Kojima, and H. Matsumoto (1994), Computer simulation of electrostatic solitary waves: A nonlinear model of broadband electrostatic noise, *Geophys. Res. Lett.*, *21*, 2923–2926.

Omura, Y., H. Matsumoto, T. Miyake, and H. Kojima (1996), Electron beam instabilities as generation mechanisms of electrostatic solitary waves in the magnetotail, *J. Geophys. Res.*, *101*, 2685–2697.

Omura, Y., H. Kojima, N. Miki, T. Mukai, H. Matsumoto, and R. Anderson (1999), Electrostatic solitary waves carried by diffusive electron beams observed by the Geotail spacecraft, *J. Geophys. Res.*, *104*, 14,627–14,637.

Onsager, T. G., M. F. Thomsen, R. C. Elphic, J. T. Gosling, R. R. Anderson, and G. Kettmann (1993), Electron generation of electrostatic waves in the plasma sheet boundary layer, *J. Geophys. Res.*, *98*, 15,509–15,520.

Parks, G. K., et al. (1984), Particle and field characteristics of the high latitude plasma sheet boundary layer, *J. Geophys. Res.*, *89*, 8885–8906.

Saeki, K., P. Michelsen, H. L. Pecseli, and J. J. Rasumussen (1979), Formation and coalescence of electron solitary holes, *Phys. Rev. Lett.*, *42*, 501–504.

Schamel, H. (1972), Stationary solitary, snoidal and sinusoidal ion acoustic waves, *Plasma Phys.*, *14*, 905–924.

Schamel, H. (1973), A modified Korteweg-de Vries equation for ion-acoustic waves due to resonant electrons, *J. Plasma Phys.*, *9*, 377–387.

Schamel, H. (1975), Analytic BGK modes and their modulational instability, *J. Plasma Phys.*, *13*, 139–145.

Schamel, H. (1979), Theory of electron holes, *Phys. Scr.*, *20*, 336–342.

Schamel, H. (1982), Stability of electron vortex structures in phase space, *Phys. Rev. Lett.*, *48*, 481–483.

Schamel, H. (1986), Electron holes, ion holes, and double layers, *Phys. Rep.*, *140*, 161–191.

Schamel, H. (2000), Hole equilibria in Vlasov-Poisson systems: A challenge to wave theories of ideal plasmas, *Phys. Plasmas*, *7*, 4831–4844.

Singh, S. V., and G. S. Lakhina (2001), Generation of electron-acoustic waves in the magnetosphere, *Planet. Space Sci.*, *49*, 107–114.

Tagare, S. G., S. V. Singh, R. V. Reddy, and G. S. Lakhina (2004), Electron acoustic solitons in the Earth's magnetotail, *Nonlinear Proc. Geophys.*, *11*, 215–218.

Temerin, M., K. Cerny, W. Lotko, and F. S. Mozer (1982), Observations of double layers and solitary waves in the auroral plasma, *Phys. Rev. Lett.*, *48*, 1175–1179.

Tokar, R. L., and S. P. Gary (1984), Electrostatic hiss and the beam driven electron acoustic instability in the dayside polar cusp, *Geophys. Res. Lett.*, *11*, 1180–1183.

Turikov, V. A. (1984), Electron phase space holes as localized BGK solutions, *Phys. Scr.*, *30*, 73–77.

Washimi, H., and T. Taniuti (1966), Propagation of ion-acoustic solitary waves of small amplitude, *Phys. Rev. Lett.*, *17*, 996–998.

Watanabe, K., and T. Taniuti (1977), Electron-acoustic mode in a plasma of two-temperature electrons, *J. Phys. Soc. Jpn.*, *43*, 1819–1820.

W. F. El-Taibany, Physics Department, Faculty of Science-Damietta, Mansoura University, Damietta El-Gedida, 34517 Egypt. (eltaibany@hotmail.com)